



# CHORUS

This is the accepted manuscript made available via CHORUS. The article has been published as:

## Strong Support for the Millisecond Pulsar Origin of the Galactic Center GeV Excess

Richard Bartels, Suraj Krishnamurthy, and Christoph Weniger

Phys. Rev. Lett. **116**, 051102 — Published 4 February 2016

DOI: [10.1103/PhysRevLett.116.051102](https://doi.org/10.1103/PhysRevLett.116.051102)

# Strong Support for the Millisecond Pulsar Origin of the Galactic Center GeV Excess

Richard Bartels,<sup>1,\*</sup> Suraj Krishnamurthy,<sup>1,†</sup> and Christoph Weniger<sup>1,‡</sup>

<sup>1</sup>*GRAPPA Institute, University of Amsterdam, Science Park 904, 1090 GL Amsterdam, Netherlands*

(Dated: December 14, 2015)

Using  $\gamma$ -ray data from the *Fermi* Large Area Telescope, various groups have identified a clear excess emission in the inner Galaxy, at energies around a few GeV. This excess resembles remarkably well a signal from dark matter annihilation. One of the most compelling astrophysical interpretations is that the excess is caused by the combined effect of a previously undetected population of dim  $\gamma$ -ray sources. Due to their spectral similarity, the best candidates are millisecond pulsars. Here, we search for this hypothetical source population, using a novel approach based on wavelet decomposition of the  $\gamma$ -ray sky and the statistics of Gaussian random fields. Using almost seven years of *Fermi*-LAT data, we detect a clustering of photons as predicted for the hypothetical population of millisecond pulsar, with a statistical significance of  $10.0\sigma$ . For plausible values of the luminosity function, this population explains 100% of the observed excess emission. We argue that other extragalactic or Galactic sources, a mismodeling of Galactic diffuse emission, or the thick-disk population of pulsars are unlikely to account for this observation.

*Introduction.* Since its launch in 2008, the *Fermi* Large Area Telescope (LAT) has revolutionized our understanding of the  $\gamma$ -ray sky. Among the major successes are the detection of more than three thousand  $\gamma$ -ray sources [1], the discovery of the *Fermi* bubbles [2], some of the most stringent limits on dark matter annihilation [3], and most recently the detection of cross-correlations between the extragalactic  $\gamma$ -ray background and various galaxy catalogues [4].

One of the most interesting  $\gamma$ -ray signatures, identified in the *Fermi*-LAT data by various groups [5–16], is an excess emission in the inner Galaxy at energies around a few GeV. This excess attracted great attention, because it has properties typical for a dark matter annihilation signal. This *Galactic center excess* (GCE) is detected both within the inner 10 arcmin of the Galactic center (GC) [7, 9, 10] and up to Galactic latitudes of more than ten degrees [13, 15, 17, 18]. It features a remarkably uniform spectrum and approximately spherical symmetry [13, 15]. Proposed diffuse emission mechanisms, like leptonic or hadronic outbursts [19–21] or cosmic-ray injection in the central molecular zone [22], potentially explain part of the excess emission. However, it is challenging to explain *all* of the above aspects of the GCE with these mechanisms alone.

The probably most plausible astrophysical interpretation for the GCE is the combined emission from a large number of unresolved millisecond pulsars (MSPs) in the Galactic bulge region [10, 12, 23, 24]. MSPs feature a spectrum compatible with the GCE emission [15], and a large unresolved component can naturally explain the uniformity of the GCE spectrum in different regions of the sky. Recently, it was shown that the spatial distribution of MSPs that were spilled out of disrupted globular clusters can explain the morphology of the GCE [25]. Such MSPs from disrupted globular clusters have also been suggested as the source behind the GeV through TeV emission in the inner few parsec of the GC [26]. Fur-

ther possible support for the MSP hypothesis might come from *Chandra* observation of low mass X-ray binaries (which are progenitor systems of MSPs) in M31, which show a centrally peaked profile in the inner 2 kpc [27, 28], as well as the recent observation of extended hard X-ray emission from the Galactic center by *NuSTAR* [29].

It was claimed that an interpretation of 100% of the GCE emission in terms of MSPs would be already ruled out: A sizeable fraction of the required  $10^3$ – $10^4$  MSPs should have been already detected by the *Fermi*-LAT [30, 31], but no (isolated) MSP has been identified so far in the bulge region. This conclusion depends, however, crucially on the adopted  $\gamma$ -ray luminosity of the brightest MSPs in the bulge population, on the effective source sensitivity of *Fermi*-LAT, and on the treatment of unassociated sources in the inner Galaxy [25, 32]. A realistic sensitivity study for MSPs in the context of the GeV excess, taking into account all these effects, was lacking in the literature up to now (but see Ref. [33]).

In this *Letter*, we close this gap and present a novel technique for the analysis of dim  $\gamma$ -ray sources, and apply it to *Fermi*-LAT observations of the inner Galaxy. Our method is based on the statistics of maxima in the wavelet-transformed  $\gamma$ -ray sky.<sup>1</sup> We search for contributions from a large number of dim MSP-like sources, assuming that they are spatially distributed like suggested by GCE observations. Our method has several advantages w.r.t. previously proposed techniques based on one-point fluctuations [34], most notably the independence from Galactic diffuse emission models, and the ability for candidate source localization.

*Modeling.* We simulate a population of MSP-like sources, henceforth simply *central source population*

---

<sup>1</sup> In context of *Fermi*-LAT data, wavelet transforms were used previously for the identification of point source seeds [1, 16]

(CSP), distributed around the GC at 8.5 kpc distance from the Sun. The CSP is taken to have a spatial distribution that follows a radial power-law with an index of  $\Gamma = -2.5$  and a hard cutoff at radius  $r = 3$  kpc [13, 15]. As reference  $\gamma$ -ray energy spectrum, we adopt the stacked MSP spectrum from Ref. [35],  $\frac{dN}{dE} \propto e^{-E/3.78 \text{ GeV}} E^{-1.57}$ . The  $\gamma$ -ray luminosity function is modeled with a power-law,  $\frac{dN}{dL} \propto L^{-\alpha}$ , with index  $\alpha = -1.5$  [32, 35–37], and with lower and upper hard cutoffs at  $L_{\min} = 10^{29} \text{ erg s}^{-1}$  and  $L_{\max} = 10^{34} - 10^{36} \text{ erg s}^{-1}$ , respectively. Luminosities are integrated over 0.1–100 GeV. Our results depend little on  $L_{\min}$ . Given that only about 70 MSPs have been detected in  $\gamma$ -rays up to now [33],  $L_{\max}$  is not well constrained. The  $\gamma$ -ray luminosity of the brightest observed MSP is somewhere in the range  $0.5 - 2 \cdot 10^{35} \text{ erg s}^{-1}$  [33, 35], depending on the adopted source distance [25, 32]. Diffuse emission is modeled with the standard model for point source analysis, `gll_iem_v06.fits`, and the corresponding isotropic background.

*Data.* For our analysis, we use almost seven years of ultraclean *Fermi*-LAT P8R2 data, taken between 4 Aug 2008 and 3 Jun 2015 (we find similar results for source class data). We select both front and back converted events in the energy range 1–4 GeV, which covers the peak of the GCE spectrum. The Region Of Interest (ROI) covers the inner Galaxy and spans Galactic longitudes  $|\ell| \leq 12^\circ$  and latitudes  $2^\circ \leq |b| \leq 12^\circ$ . The data is binned in Cartesian coordinates with a pixel size of  $0.1^\circ$ .

*Wavelet peaks.* The wavelet transform of the  $\gamma$ -ray data is defined as the convolution of the photon count map,  $\mathcal{C}(\Omega)$ , with the wavelet kernel,  $\mathcal{W}(\Omega)$ ,

$$\mathcal{F}_{\mathcal{W}}[\mathcal{C}](\Omega) \equiv \int d\Omega' \mathcal{W}(\Omega - \Omega') \mathcal{C}(\Omega'), \quad (1)$$

where  $\Omega$  denotes Galactic coordinates [38] (note that  $\int d\Omega \mathcal{W}(\Omega) = 0$ ). The central observable for the current analysis is the *signal-to-noise ratio* (SNR) of the wavelet transform, which we define as

$$\mathcal{S}(\Omega) \equiv \frac{\mathcal{F}_{\mathcal{W}}[\mathcal{C}](\Omega)}{\sqrt{\mathcal{F}_{\mathcal{W}^2}[\mathcal{C}](\Omega)}}, \quad (2)$$

where in the denominator the wavelet kernel is squared before performing the convolution. If the  $\gamma$ -ray flux varied only on scales much larger than the extent of the wavelet kernel, and in the limit of a large number of photons,  $\mathcal{S}(\Omega)$  would behave like a smoothed Gaussian random field. *Consequently,  $\mathcal{S}(\Omega)$  can be loosely interpreted as the local significance for having a source at position  $\Omega$ , in units of standard deviations.*

As wavelet kernel, we adopt the second member of the Mexican Hat Wavelet Family, MHWF2, which was shown to provide very good source discrimination power [39], and which was used for identification of compact sources

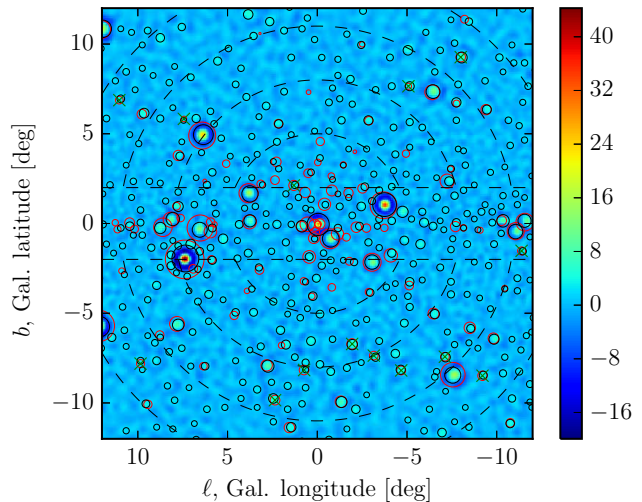


FIG. 1. SNR of the wavelet transform of  $\gamma$ -rays with energies in the range 1–4 GeV,  $\mathcal{S}(\Omega)$ . The black circles show the position of wavelet peaks with  $\mathcal{S} \geq 2$ ; the red circles show the position of 3FGL sources. In both cases, the circle area scales with the significance of the source detection in that energy range. The dashed lines indicate the regions that we use for the binned likelihood analysis, where latitudes  $|b| < 2^\circ$  are excluded because of the strong emission from the Galactic disk. The subset of 3FGL sources that remains unmasked in our analysis is indicated by the green crosses.

in Planck data [40]. The wavelet can be obtained by a successive application of the Laplacian operator to a two-dimensional Gaussian distribution with width  $\sigma_b \cdot R$ . Here,  $\sigma_b = 0.4^\circ$  corresponds to the *Fermi*-LAT angular resolution at 1–4 GeV, and  $R$  is a tuning parameter. We find best results when  $R$  varies linearly with latitude from  $R = 0.53$  at  $b = 0^\circ$  to  $R = 0.83$  at  $b = \pm 12^\circ$ . This compensates to some degree the increasing diffuse backgrounds towards the Galactic disk, while optimizing the source sensitivity at higher latitudes [40].

The resulting SNR of the wavelet transform,  $\mathcal{S}(\Omega)$ , is shown in Fig. 1. As expected, the Galactic diffuse emission is almost completely filtered out by the wavelet transform, whereas bright sources lead to pronounced peaks. We adopt a simple algorithm for peak identification: We find all pixels in  $\mathcal{S}(\Omega)$  with values larger than in the four adjacent pixels. We then clean these results from artefacts by forming clusters of peaks with coplanar distances less than  $0.3^\circ$ , and only keep the most significant peak in each cluster.

In Fig. 1, we show the identified wavelet peaks with peak significance  $\mathcal{S} > 2$ , as well as all 3FGL sources for comparison [1]. For sources that are bright enough in the adopted energy range, we find a good correspondence between wavelet peaks and the 3FGL, both in terms of position and significance (we compare the significance of wavelet peaks,  $\mathcal{S}$ , with the 1–3 GeV detection significance

for 3FGL sources).

It is worth emphasizing that *for the adopted spherically symmetric and centrally peaked distribution of the CSP, most of the sources would be detected not directly at the GC, but a few degrees away from the Galactic disk.* This is simply due to the much weaker diffuse emission at higher latitudes. Our focus on latitudes  $|b| \geq 2^\circ$  thus avoids regions where source detection becomes less efficient, due to strong diffuse foregrounds, without significant sensitivity loss for the source population of interest.

*3FGL sources.* Before studying the statistics of the wavelet peaks in detail below, we remove almost all peaks that correspond to known 3FGL sources based on a  $0.3^\circ$  ( $1^\circ$  for  $\sqrt{TS} \geq 50$ ) proximity cut. However, in order to mitigate a potential bias on  $L_{\max}$ , we do not mask peaks that correspond to 3FGL sources that are likely part of the CSP. We identify such *MSP candidate sources* by requiring that they (i) are tagged as unassociated, (ii) show no indication for variability and (iii) have a spectrum compatible with MSPs. The last criterion is tested by performing a  $\chi^2$ -fit of the above MSP reference spectrum to the spectrum given in the 3FGL (0.1–100 GeV; five energy bins). Only the normalization is left free to vary. We require a fit quality of  $\chi^2/\text{dof} \leq 1.22$  (with  $\text{dof}=4$ ), corresponding to a  $p$ -value  $\geq 0.3$ .

We find 13 3FGL source in the inner Galaxy ROI that pass the above MSP cuts (listed in the supplementary material). Interestingly, the average number of MSP candidate sources in same-sized control regions along the Galactic disk in the range  $|\ell| = 12^\circ$ – $60^\circ$  is significantly smaller, with an average of 3.1. It is tempting to interpret this excess of MSP candidate sources in the inner Galaxy as being caused by the brightest sources of the CSP, above the less pronounced thick-disk population of MSPs [41, 42]. However, we emphasize that the status of these 13 sources is currently neither clear, nor qualitatively decisive for our results. Whether we mask them plays a minor role for the detection of the CSP below (but does affect the inferred values for  $L_{\max}$ , see supplementary material).

*Statistical analysis.* In Fig. 2 we show a histogram of the wavelet peaks in our ROI. We bin the peaks in a two-dimensional grid, which spans the projected Galactocentric angle  $2^\circ$ – $17^\circ$ , and wavelet peak significances in the range 1–10. The bin edges are as indicated in the figure. As expected, photon shot noise gives rise to a large number of peaks with low significances  $\mathcal{S} \leq 3$ , and only a small number of peaks has  $\mathcal{S} \geq 5$ .

We assume that the number of peaks in each bin in Fig. 2 follows – in repeated experiments and random realizations of the CSP – to a good approximation a Poisson distribution. We estimate the corresponding average number of expected wavelet peaks in each bin using a large number of Monte Carlo (MC) simulations, where we simulate the diffuse background emission, random re-

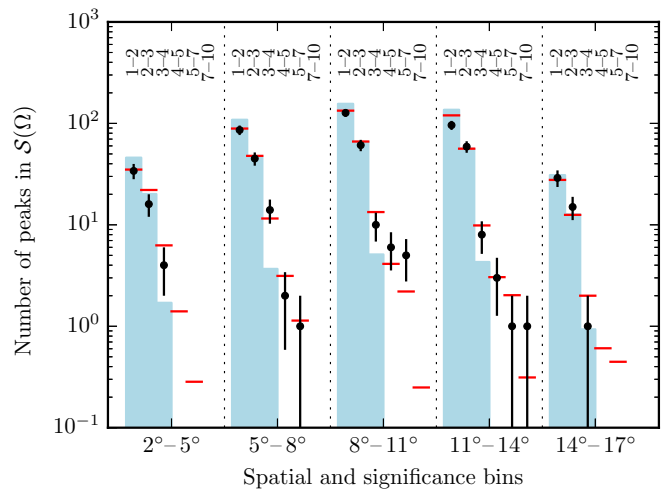


FIG. 2. Histogram of observed peaks in  $\mathcal{S}(\Omega)$ , in bins of projected radial distance from the GC and SNR values (black dots with statistical error bars). We show the expectation value for the case of a negligible CSP as blue bars, whereas the expectation values for the best-fit are shown in red.

alizations of the source population and photon shot noise.

In order to quantify what CSP luminosity function reproduces best the observations, we perform a binned Poisson likelihood analysis of the wavelet peak distribution. The likelihood function is given by

$$\mathcal{L} = \prod_{i=1}^{n_r} \prod_{j=1}^{n_s} \mathcal{P}(c_{ij} | \mu_{ij}(L_{\max}, \Phi_5)), \quad (3)$$

where  $n_r$  and  $n_s$  are respectively the numbers of radial and peak SNR bins,  $c_{ij}$  are the observed and  $\mu_{ij}$  the expected number of peaks, and  $\mathcal{P}$  is a Poisson distribution. The expectation values depend directly on the maximal luminosity,  $L_{\max}$ , as well as on the number of simulated sources,  $n$ . To ease comparison with the literature, we determine  $n$  as a function of  $\Phi_5$ , which denotes the mean differential intensity of the CSP at  $b = \pm 5^\circ$ ,  $\ell = 0^\circ$  and 2 GeV. In the case of the GCE, this value was found to be  $\Phi_5^{\text{GCE}} = (8.5 \pm 1.5) \times 10^{-7} \text{ GeV}^{-1} \text{ cm}^{-2} \text{ s}^{-1} \text{ sr}^{-1}$  at 95.4% CL [15].

*Results.* In Fig. 2, we show the expectation values that we obtain when neglecting contributions from the CSP (and any other non-diffuse emission). This corresponds to good approximation to the case where the GCE is of truly diffuse origin, including the case of DM annihilation or outburst events. We find that the observed number of wavelet peaks with  $\mathcal{S} < 2$  is significantly lower than expected, whereas the observed number of peaks with  $\mathcal{S} > 3$  is significantly higher. As we will show next, *this is precisely the effect that is caused by a dim source population.*

We now turn to the case with a non-zero CSP contribution. In Fig. 3, we show the limits that we obtain on the

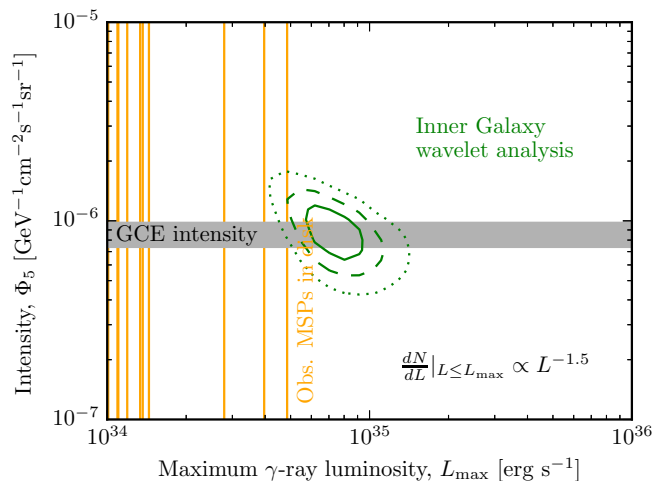


FIG. 3. Constraints on the maximum  $\gamma$ -ray luminosity of the CSP,  $L_{\max}$ , and the population averaged intensity at  $b = \pm 5^\circ$ ,  $\ell = 0^\circ$  and 2 GeV,  $\Phi_5$ , as derived from our wavelet analysis. We show 68.7%, 95.4% and 99.7% CL contours. We also indicate the values of  $\Phi_5$  where the source population can explain 100% of the GCE (horizontal gray band, 95.4% CL), and as vertical orange lines the luminosity of the brightest observed nearby MSPs.

two CSP parameters when fitting the histogram in Fig. 2 as described above. We find that a non-zero contribution from the CSP is favoured at the level of at least  $10.0\sigma$ .<sup>2</sup> The best-fit value for the total differential intensity is  $\Phi_5 = (9.0 \pm 1.9) \times 10^{-7} \text{ GeV}^{-1} \text{ cm}^{-2} \text{ s}^{-1} \text{ sr}^{-1}$  and for the maximum luminosity  $L_{\max} = (7.0 \pm 1.0) \times 10^{34} \text{ erg s}^{-1}$ . As can be seen in Fig. 2, we obtain in this case a very good fit to the data.

Our preferred range of the maximum  $\gamma$ -ray luminosities reaches up to  $L_{\max} \leq 1.04 \times 10^{35} \text{ erg s}^{-1}$  (at 95.4% CL), which is compatible with observations of nearby MSPs. We illustrate this by showing in Fig. 3 the  $\gamma$ -ray luminosity of the brightest individually observed nearby MSPs as given in Ref. [35].<sup>3</sup> Furthermore, for the adopted slope of the luminosity function,  $\alpha = 1.5$ , the best-fit value for the total differential intensity of the CSP,  $\Phi_5$ , is consistent with the CSP accounting for 100% of the GCE emission.

*Discussion and conclusions.* We found corroborating evidence for the hypothesis that the GCE is caused by a hitherto undetected population of MSP-like sources. We performed a wavelet transform of the  $\gamma$ -ray emission

from the inner Galaxy, which removes Galactic diffuse emission and enhances point sources, and we studied the statistics of the peaks in this transform. We detected with  $10.0\sigma$  significance a suppression (enhancement) of low (high)-significance wavelet peaks, relative to the expectations for purely diffuse emission. We showed that this effect is caused by the presence of a large number of dim point sources. The spatial distribution of wavelet peaks in the inner Galaxy is compatible with a centrally peaked source distribution, and the inferred cutoff of the  $\gamma$ -ray luminosity function of these sources agrees with the observation of nearby MSPs. This source population can, for reasonable slopes of the luminosity function, account for 100% of the GCE emission.

For the purpose of this *Letter*, which introduces a novel technique, we kept our analysis as simple as possible. In general, one might worry that our results could be affected by the presence of extragalactic and Galactic sources, by the thick-disk population of MSPs and young pulsars, by the details of masking and unmasking 3FGL sources, by the details of the adopted  $\gamma$ -ray luminosity function, and by unmodeled substructure in the Galactic diffuse emission that is not removed by the wavelet transform. We address all of these points in the supplementary material and show that it is rather unlikely that they affect our results qualitatively, although quantitative changes in the obtained best-fit values for  $\Phi_5$  and  $L_{\max}$  are possible. In particular, we show that the wavelet signal expected from the thick-disk population of MSPs is an order of magnitude weaker than what we actually observe, and that interpretations related to unmodeled gas remain on closer inspection unlikely.

The prospects for fully establishing the MSP interpretation within the coming decade are very good. Our results suggest that upcoming  $\gamma$ -ray observations with improved angular resolution (planned/proposed  $\gamma$ -ray satellites like GAMMA-400 [43], ASTROGAM and PANGU [44]) will allow to detect many more of the bulge sources, and to study their distribution and spectra. For current radio instruments, it remains rather challenging to detect a MSP population in the bulge [25], but prospects for next-generation instruments are good.

*Acknowledgments.* We thank for useful discussions with David Berge, Francesca Calore, Ilias Cholis, Jennifer Gaskins, Dan Hooper, Simona Murgia, Tracy Slatyer, Ben Safdi and Jacco Vink. We thank the *Fermi* collaboration for providing the public *Fermi* data as well as the *Fermi* Science Tools (v10r0p5). SURFsara is thanked for use of the Lisa Compute Cluster. SK and CW (P.I.) are part of the VIDI research programme “Probing the Genesis of Dark Matter”, which is financed by the Netherlands Organisation for Scientific Research (NWO). RB is part of a GRAPPA-PhD program funded by NWO. Part of this work was performed at the Aspen Center for Physics, which is supported by National Science Foundation grant PHY-1066293.

<sup>2</sup> When quoting the statistical significance, we conservatively take into account bins with  $S < 5$  only, which are most affected by a dim source population, and least affected by the masking of 3FGL sources (see supplementary material for details).

<sup>3</sup> We only show objects where 2PC [33] distances are available; see Ref. [25] for a detailed discussion about distance uncertainties.

- 
- \* r.t.bartels@uva.nl  
† s.krishnamurthy@uva.nl  
‡ c.weniger@uva.nl
- [1] The Fermi-LAT Collaboration, ArXiv e-prints (2015), arXiv:1501.02003 [astro-ph.HE].
  - [2] M. Su, T. R. Slatyer, and D. P. Finkbeiner, *Astrophys. J.* **724**, 1044 (2010), arXiv:1005.5480 [astro-ph.HE].
  - [3] M. Ackermann *et al.* (Fermi-LAT), (2015), arXiv:1503.02641 [astro-ph.HE].
  - [4] J.-Q. Xia, A. Cuoco, E. Branchini, and M. Viel, *Astrophys.J.Suppl.* **217**, 15 (2015), arXiv:1503.05918 [astro-ph.CO].
  - [5] L. Goodenough and D. Hooper, (2009), arXiv:0910.2998 [hep-ph].
  - [6] V. Vitale and A. Morselli (Fermi/LAT Collaboration), (2009), arXiv:0912.3828 [astro-ph.HE].
  - [7] D. Hooper and L. Goodenough, *Phys.Lett.* **B697**, 412 (2011), arXiv:1010.2752 [hep-ph].
  - [8] D. Hooper and T. Linden, *Phys.Rev.* **D84**, 123005 (2011), arXiv:1110.0006 [astro-ph.HE].
  - [9] K. N. Abazajian and M. Kaplinghat, *Phys.Rev.* **D86**, 083511 (2012), arXiv:1207.6047 [astro-ph.HE].
  - [10] C. Gordon and O. Macias, *Phys.Rev.* **D88**, 083521 (2013), arXiv:1306.5725 [astro-ph.HE].
  - [11] O. Macias and C. Gordon, *Phys.Rev.* **D89**, 063515 (2014), arXiv:1312.6671 [astro-ph.HE].
  - [12] K. N. Abazajian, N. Canac, S. Horiuchi, and M. Kaplinghat, *Phys.Rev.* **D90**, 023526 (2014), arXiv:1402.4090 [astro-ph.HE].
  - [13] T. Daylan, D. P. Finkbeiner, D. Hooper, T. Linden, S. K. N. Portillo, *et al.*, (2014), arXiv:1402.6703 [astro-ph.HE].
  - [14] B. Zhou, Y.-F. Liang, X. Huang, X. Li, Y.-Z. Fan, *et al.*, (2014), arXiv:1406.6948 [astro-ph.HE].
  - [15] F. Calore, I. Cholis, and C. Weniger, *JCAP* **1503**, 038 (2015), arXiv:1409.0042 [astro-ph.CO].
  - [16] M. Ajello *et al.* (Fermi-LAT), (2015), arXiv:1511.02938 [astro-ph.HE].
  - [17] D. Hooper and T. R. Slatyer, *Phys.Dark Univ.* **2**, 118 (2013), arXiv:1302.6589 [astro-ph.HE].
  - [18] W.-C. Huang, A. Urbano, and W. Xue, (2013), arXiv:1307.6862 [hep-ph].
  - [19] E. Carlson and S. Profumo, *Phys.Rev.* **D90**, 023015 (2014), arXiv:1405.7685 [astro-ph.HE].
  - [20] J. Petrovic, P. D. Serpico, and G. Zaharijas, *JCAP* **1410**, 052 (2014), arXiv:1405.7928 [astro-ph.HE].
  - [21] I. Cholis, C. Evoli, F. Calore, T. Linden, C. Weniger, and D. Hooper, (2015), arXiv:1506.05119 [astro-ph.HE].
  - [22] D. Gaggero, M. Taoso, A. Urbano, M. Valli, and P. Ullio, (2015), arXiv:1507.06129 [astro-ph.HE].
  - [23] K. N. Abazajian, *JCAP* **1103**, 010 (2011), arXiv:1011.4275 [astro-ph.HE].
  - [24] Q. Yuan and B. Zhang, *JHEAp* **3-4**, 1 (2014), arXiv:1404.2318 [astro-ph.HE].
  - [25] T. D. Brandt and B. Kocsis, (2015), arXiv:1507.05616 [astro-ph.HE].
  - [26] W. Bednarek and T. Sobczak, *Mon. Not. Roy. Astron. Soc.* **435**, L14 (2013), arXiv:1306.4760 [astro-ph.HE].
  - [27] R. Voss and M. Gilfanov, *Astron. and Astroph.* **468**, 49 (2007), astro-ph/0610649.
  - [28] K. N. Abazajian and M. Kaplinghat, *Phys. Rev. D* **86**, 083511 (2012), arXiv:1207.6047 [astro-ph.HE].
  - [29] K. Perez, C. J. Hailey, F. E. Bauer, R. A. Krivonos, K. Mori, F. K. Baganoff, N. M. Barrière, S. E. Boggs, F. E. Christensen, W. W. Craig, B. W. Grefenstette, J. E. Grindlay, F. A. Harrison, J. Hong, K. K. Madsen, M. Nynka, D. Stern, J. A. Tomsick, D. R. Wik, S. Zhang, W. W. Zhang, and A. Zoglauer, *Nature (London)* **520**, 646 (2015).
  - [30] D. Hooper, I. Cholis, T. Linden, J. Siegal-Gaskins, and T. Slatyer, *Phys.Rev.* **D88**, 083009 (2013), arXiv:1305.0830 [astro-ph.HE].
  - [31] I. Cholis, D. Hooper, and T. Linden, (2014), arXiv:1407.5625 [astro-ph.HE].
  - [32] J. Petrović, P. D. Serpico, and G. Zaharijas, *JCAP* **1502**, 023 (2015), arXiv:1411.2980 [astro-ph.HE].
  - [33] A. Abdo *et al.* (The Fermi-LAT collaboration), *Astrophys.J.Suppl.* **208**, 17 (2013), arXiv:1305.4385 [astro-ph.HE].
  - [34] S. K. Lee, M. Lisanti, and B. R. Safdi, *JCAP* **1505**, 056 (2015), arXiv:1412.6099 [astro-ph.CO].
  - [35] I. Cholis, D. Hooper, and T. Linden, (2014), arXiv:1407.5583 [astro-ph.HE].
  - [36] A. W. Strong, *Astrophys.Space Sci.* **309**, 35 (2007), arXiv:astro-ph/0609359 [astro-ph].
  - [37] C. Venter, T. Johnson, A. Harding, and J. Grove, (2014), arXiv:1411.0559 [astro-ph.HE].
  - [38] F. Damiani, A. Maggio, G. Micela, and S. Sciortino, *The Astrophysical Journal* **483**, 350 (1997).
  - [39] J. Gonzalez-Nuevo, F. Argüeso, M. Lopez-Cañiego, L. Toffolatti, J. Sanz, *et al.*, *Mon.Not.Roy.Astron.Soc.* **369**, 1603 (2006), arXiv:astro-ph/0604376 [astro-ph].
  - [40] P. Ade *et al.* (Planck), *Astron.Astrophys.* **571**, A28 (2014), arXiv:1303.5088 [astro-ph.CO].
  - [41] T. Gregoire and J. Knödseder, (2013), arXiv:1305.1584 [astro-ph.GA].
  - [42] F. Calore, M. Di Mauro, F. Donato, and F. Donato, *Astrophys.J.* **796**, 1 (2014), arXiv:1406.2706 [astro-ph.HE].
  - [43] N. Topchiev, A. Galper, V. Bonvicini, O. Adriani, R. Aptekar, *et al.*, *Bull.Russ.Acad.Sci.Phys.* **79**, 417 (2015).
  - [44] X. Wu, M. Su, A. Bravar, J. Chang, Y. Fan, *et al.*, *Proc.SPIE Int.Soc.Opt.Eng.* **9144**, 91440F (2014), arXiv:1407.0710 [astro-ph.IM].